

Received: 2019.12.29  
Accepted: 2020.02.28  
Available online: 2020.04.06  
Published: 2020.06.15

# Comparative Three-Dimensional Finite Element Analysis of 4 Kinds of Pedicle Screw Schemes for Treatment of Adult Degenerative Scoliosis

Authors' Contribution:  
Study Design A  
Data Collection B  
Statistical Analysis C  
Data Interpretation D  
Manuscript Preparation E  
Literature Search F  
Funds Collection G

ABE 1 **Yang Zhou**  
CD 2 **Daqi Xin**  
C 3 **Zhuoting Lei**  
CD 4 **Yuan Zuo**  
EG 4 **Yan Zhao**

1 Graduate School of Inner Mongolia Medical University, Hohhot, Inner Mongolia, P.R. China  
2 Department of Thoracic and Lumbar Spine Surgery, Second Affiliated Hospital of Inner Mongolia Medical University, Hohhot, Inner Mongolia, P.R. China  
3 College of Traditional Chinese Medicine, Inner Mongolia Medical University, Hohhot, Inner Mongolia, P.R. China  
4 Department of Laboratory Medicine, Second Affiliated Hospital of Inner Mongolia Medical University, Hohhot, Inner Mongolia, P.R. China

**Corresponding Authors:** Yan Zhao, e-mail: [nmgzy4568@126.com](mailto:nmgzy4568@126.com), Yuan Zuo, e-mail: [2574893233@qq.com](mailto:2574893233@qq.com)

**Source of support:** This study was supported by the National Natural Science Foundation of China (No: 81441057) and the Inner Mongolia Natural Science Foundation (No: 2016MS08132)

**Background:** This study aimed to evaluate the biomechanical stress of the internal fixation screws and vertebral bodies after the full-segment, interval, key vertebral, and strategy pedicle screw fixations under 7 work conditions in a patient with adult degenerative scoliosis (ADS) using finite elements (FE) analysis.

**Material/Methods:** A patient with ADS underwent internal fixation by pedicle screws after posterior incision in combination with subtotal laminectomy decompression and bone graft fusion, and received thin-layer computed tomography (CT) spine scanning at T12–L5. The CT data were used to constitute three-dimensional FE full-segment, interval, key vertebral, and strategic pedicle screw models. The stress of each screw-rod system under different working conditions was evaluated.

**Results:** Forward flexion, backward extension, lateral flexion, and rotation greatly increased the force of the pedicle screw systems. The maximum stress of the screw-rods was the lowest in the full-segment model under almost all the working conditions except for the upright situation. The maximum stress of the vertebral bodies was the minimum in the strategic model under all the 7 working conditions, followed by that in the key vertebra and full-segment models.

**Conclusions:** Collectively, the strategic and key vertebra pedicle screw schemes can decrease the biomechanical stress of screw-rod systems and vertebral bodies, which is close to the full-segment scheme. Our results may help explore the optimal surgical means for pedicle screw fixation for ADS patients, which can maximally reduce the risk of screws-related postoperative complications and simultaneously maintain a reasonable 3D orthopedic effect.

**MeSH Keywords:** **Biomechanical Phenomena • Bone Screws • Finite Element Analysis Invertebrates • Scoliosis**

**Full-text PDF:** <https://www.medscimonit.com/abstract/index/idArt/922050>



## Background

Adult scoliosis is a spinal deformity occurring in adults, with a coronal deviation of Cobb angle over 10°. Adult degenerative scoliosis (ADS) is an important type of adult scoliosis, which is due to the degeneration of spinal motion segments [1]. ADS leads to global spinal imbalance, back pain, and neurological deficits, which severely influences patient quality of life. ADS is closely related to aging and typically appears in patients older than 40 years [1]. ADS has a high prevalence of about 35–68% in the elderly [2,3]. As China has the largest population in the world and is becoming an aging society, the number of ADS patients (especially elderly patients) is gradually increasing. ADS has become not only a health problem for patients, but also imposes a heavy burden on society in China.

Posterior spinal canal decompression and internal fixation is currently the most widely used surgical procedure. It consists of short- and long-segment fixation strategies, according to the numbers of fixed segments, and the choice of short- or long-segment fixation has become an important topic [4–6]. Long-segment fixation may be better to achieve satisfactory orthopedic outcome and decreases the progression of postoperative degeneration [4], but it has disadvantages such as long operation time, large blood loss, and more postoperative complications [5–7]. Moreover, some reports showed that short and long fusions achieved similar reduction in coronal Cobb angle and increase in lumbar lordosis [5,7]. To obtain satisfactory results and decrease the risks of postoperative complications (e.g., pedicle screws-based soft tissue and neural injury and infection), optimized pedicle screw strategies using fewer screws (i.e., selective screwing) have been developed and used.

Selective pedicle screw strategies have been widely used in the treatment of adolescent idiopathic scoliosis, with good results, and the bleeding, surgical time, postoperative complications can also be effectively controlled [8–11], but they have rarely been used in ADS. ADS is different from adolescent idiopathic scoliosis; for example, many patients with ADS are elderly and have special problems such as formation of an intervertebral bone bridge, decreased body flexibility, and osteoporosis. Whether selective pedicle screw schemes can be successfully used for ADS needs further study.

Optimized pedicle screw schemes for ADS surgery requires accurate biomechanical analysis of various surgical procedures. To do this, animal experiments and cadaver specimen analysis are usually needed. However, animal (especially small animal) spines are substantially different from human spines in actual anatomical structures. The imaging characteristics of cadaver specimens after treatment are also unlike those of living patients. Digital orthopedic three-dimensional (3D) finite element (FE) analysis is a promising new method for

studying spine biomechanics and it has been used to analyze the biomechanical parameters internal to spines and connective soft tissues, which are difficult to capture by experimental approaches. Moreover, even in the presence of cross-linking, which can influence the biomechanical analysis, the spine biomechanics still can be evaluated through software-based FE analysis [12,13]. Few studies have performed biomechanical analysis of ADS using FE analysis. For example, Haddas et al. established an FE model to observe the effect of adjacent load transfer on the mechanical function of the lumbar scoliotic spine [14]. Xu et al. used FE analysis to observe the increased vibrational response of the scoliotic spines in patients with ADS [15]. Wang et al. used FE models to show that, in response to the asymmetric loading, compressive deformation of facet joints appears on the concave side, which accelerates asymmetry in the lumbar spine and is related to degenerative lumbar scoliosis [16]. Zheng et al. imported spiral computed tomography (CT) scanning data on an ADS patient's lumbar spine (T12 to S1) and built and validated an integral 3D FE model of ADS to accurately simulate the physical features of ADS [17]. However, there have been no studies using FE analysis to evaluate the biomechanical characteristics of pedicle screw schemes for ADS.

The present study used FE methods to analyze the biomechanical stress of the internal fixation screws and vertebral bodies of full-segment, interval, key vertebra, and strategic pedicle screw systems under different loading conditions in a patient with ADS. Our results will help select optimal pedicle screw schemes for the treatment of ADS.

## Material and Methods

### Patient

A 60-year-old male patient was admitted in October 2017 at the Second Affiliated Hospital of Inner Mongolia Medical University (Hohhot, China). He mainly complained low back pain with right lower-extremity pain lasting for 4 years. After receiving a front and lateral full spine X-ray examination, he was diagnosed with ADS (T12–L5), with Cobb angle of 40°, lumbar motion of 34° for forward flexion and 25° for backward extension, left lateral bending of 27°, right lateral bending of 28°, left axial rotation of 35°, and right axial rotation of 37°. Nuclear magnetic imaging excluded the existence of conditions such as congenital dysplasia of the spinal cord and idiopathic scoliosis. The patient underwent internal fixation (full-segment) with pedicle screws after a posterior incision in combination with subtotal laminectomy decompression and bone graft fusion. The patient only manifested characteristics of hypertrophy of the yellow ligament, without protrusion of intervertebral disc, at L5/S1. Moreover, because of

the physiological curvature at L5/S1, screwing at these segments would greatly increase the stress of the screw-rods at L5/S1, which might decrease the stability of screw-rods and influence the treatment efficacy of ADS. Therefore, fusion was stopped at L5 in this patient.

The patient then received thin-layer CT scanning at T12–L5 spine using a 64-slice CT scanner (GE Healthcare, Waukesha, WI, USA) with a layer thickness of 1 mm. Two hundred and sixty CT images were obtained and saved in Digital Imaging and Communications in Medicine (DICOM) format.

### FE analysis

Generally, CT imaging data of the patient after the operation were collected and imported and established a full-segment pedicle screw model and secondary interval, key vertebra, and strategic pedicle screw models using Mimics software. After optimization using Geomagic software, the FE models were established using Ansys software. Then, the 4 established pedicle screw models were subject to biomechanical analysis under 7 different working conditions.

#### *Reconstruction of postoperative spinal model of ADS patient with Materialise Interactive Medical Image Control System (Mimics)17.0 software*

The CT images in DICOM format were imported by Mimics17.0 software (Materialise, Inc., Leuven, Belgium) and were then generated into coronal and sagittal view images. Using the Cropmask function of Mimics17.0 software, each part of the spine and screw-rod systems was distinguished according to difference of the gray values of the CT images. The Mask Edit function was used to manually erase the excess tissue and artifacts and fill the empty cavity. Using the Caculate 3D tool, the corresponding 3D vertebral body was obtained (Figure 1A).

To obtain better model quality to facilitate the subsequent FE analysis, the established model was properly smoothed by means of the Mimics' Remesh function, with a smoothing factor of 0.1 and 100 iterations. The final 3D model was obtained, which was saved in Standard Tessellation Language (STL) format (Figure 1B).

Establishment of the screw-rod systems. Since the gray values of the screw-rod systems and the spine were different, they were adjusted and screened to obtain a suitable gray value range of the screw-rod systems. Following the above steps, each of the screw-rods was extracted and the model was established and smoothed (Figure 1C), which was further smoothed and subject to surface mesh processing using the Remesh function. The screw-rod models were saved in STL format.

#### *Establishment of a 3D model of lumbar intervertebral discs.*

Since the gray values of the intervertebral discs and muscles around the vertebral bodies were similar, it was difficult to extract those of the intervertebral discs directly using CT data. Therefore, the Mimics splitting tool was used to roughly determine the contour of the discs on the upper and lower surfaces of the vertebral bodies, and then the Boolean operations were used to generate a solid 3D shape (Figure 1D). Of note, to exclude the interference of the fusion device and the intervertebral fusion on the overall force of the screw-rods and the force of the vertebral bodies, the fusion device was also simulated as the intervertebral discs. Similarly, the model was further smoothed and underwent surface mesh processing using the Remesh function, which was saved in STL format.

#### *Establishment of a 3D ligament model*

Similarly, it was difficult to extract the gray values of the ligament directly using CT data due to the similarity of the gray values of muscles around ligaments. According to the position and actual shape of the ligaments, the Mask Edit function was used for manual filling, and the final ligament model was prepared by using the above extraction and processing method for establishment of the vertebral body model. The model was further smoothed and underwent surface mesh processing using the Remesh function, which was saved in STL format. This study used solid ligament in the model establishment for consideration of maximal simulation of the physical structure of ligaments and accurate evaluation of the actual application in the force analysis.

#### *Secondary establishment of the interval, key vertebra, and strategic pedicle screw models*

Following the above method, the interval, key vertebra, and strategic pedicle screw models were established. For the full-segment pedicle screw scheme, both sides of the pedicle of the vertebral arch of each vertebral body within the fixed segments were screwed. For the interval scheme, those of every other vertebral body within the fixed segments were screwed. For the key vertebra scheme, the upper and lower ends of the fixed vertebrae were determined and the orthopedic side (concave side) of the apical vertebra was screwed, which was used as a reference to place a screw in the opposite side of the ipsilateral interval key vertebra until the upper and lower ends of the fixed vertebrae were reached. For the strategic scheme, a pair of screws were placed in the upper and lower ends of the vertebra, a screw was placed in the convex side of the apical vertebra, and simultaneously a screw was placed in the concave side of the upper and lower vertebral bodies adjacent to the apical vertebra. The finally assembled models are shown in Figure 1E–1H.

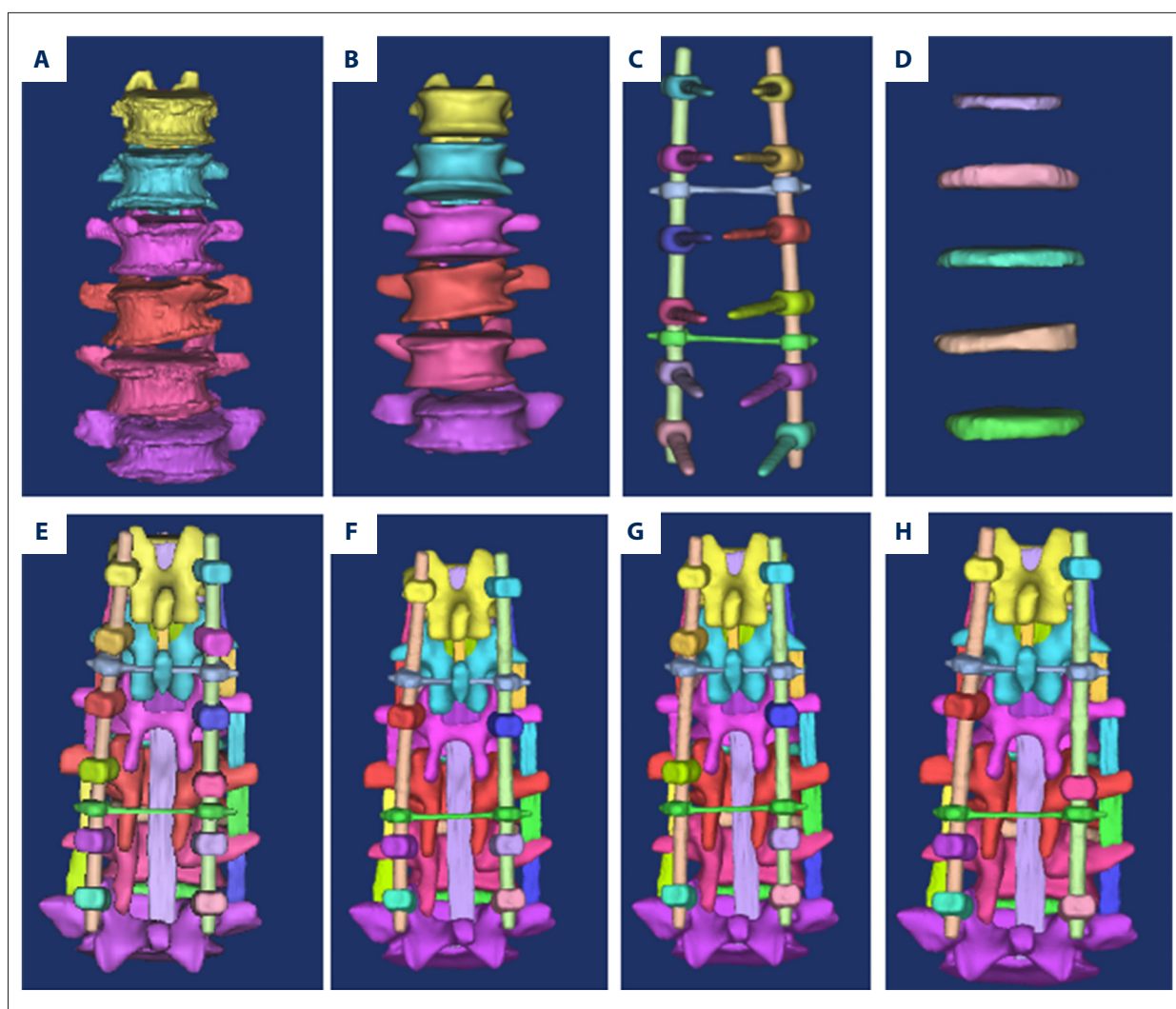


**Figure 1.** Reconstruction of postoperative spinal model of ADS patient with Mimics17.0. (A) Primary 3D vertebral body model by Mimics17.0 software. (B) Final 3D vertebral body model by the Mimics' Remesh function. (C) Establishment of 3D screw-rod system. (D) Establishment of a 3D model of lumbar intervertebral discs. (E–H). Primary full-segment (E), interval (F), key vertebra (G) and strategic (H) screw models.

### Geomagic reverse processing

The above STL files exported from Mimics software were imported into Geomagic Studio 12.0 software (Geomagic, Rock Hill, SC, USA) for further processing. The “model volume” tool of the software was used to automatically detect whether the model had a void. If so, the “fill hole” command would be selected to automatically search and fill it in the existing model. Afterward, the “sandpaper, slack” tool of the software was used to polish the sharp protrusions of the model to make it locally smooth. However, excessive slickness should not be pursued during polishing and relaxation process to avoid serious local distortion-induced losing of authenticity of models. Then, the Refine Polygon tool was used to further optimize the quality of the model's triangle polygon. Finally, the Boolean

operation function was used to remove the interference between tissues to maintain the integrity and actual similarity of the tissues. The optimized model is shown in Figure 2A–2D, where the typical structure of each segment of the vertebrae and intervertebral discs can be seen, with smooth surface and without convex sharp angle, which was more suitable for subsequent FE analysis.

### Processing using Ansys software

The above-established vertebral bodies, screw-rods, discs, ligaments, and other models were further assembled and subject to tetrahedral meshing using Ansys software (Ansys Inc., Canonsburg, PA, USA). The material properties were assigned to the models using Ansys. We used the currently internationally

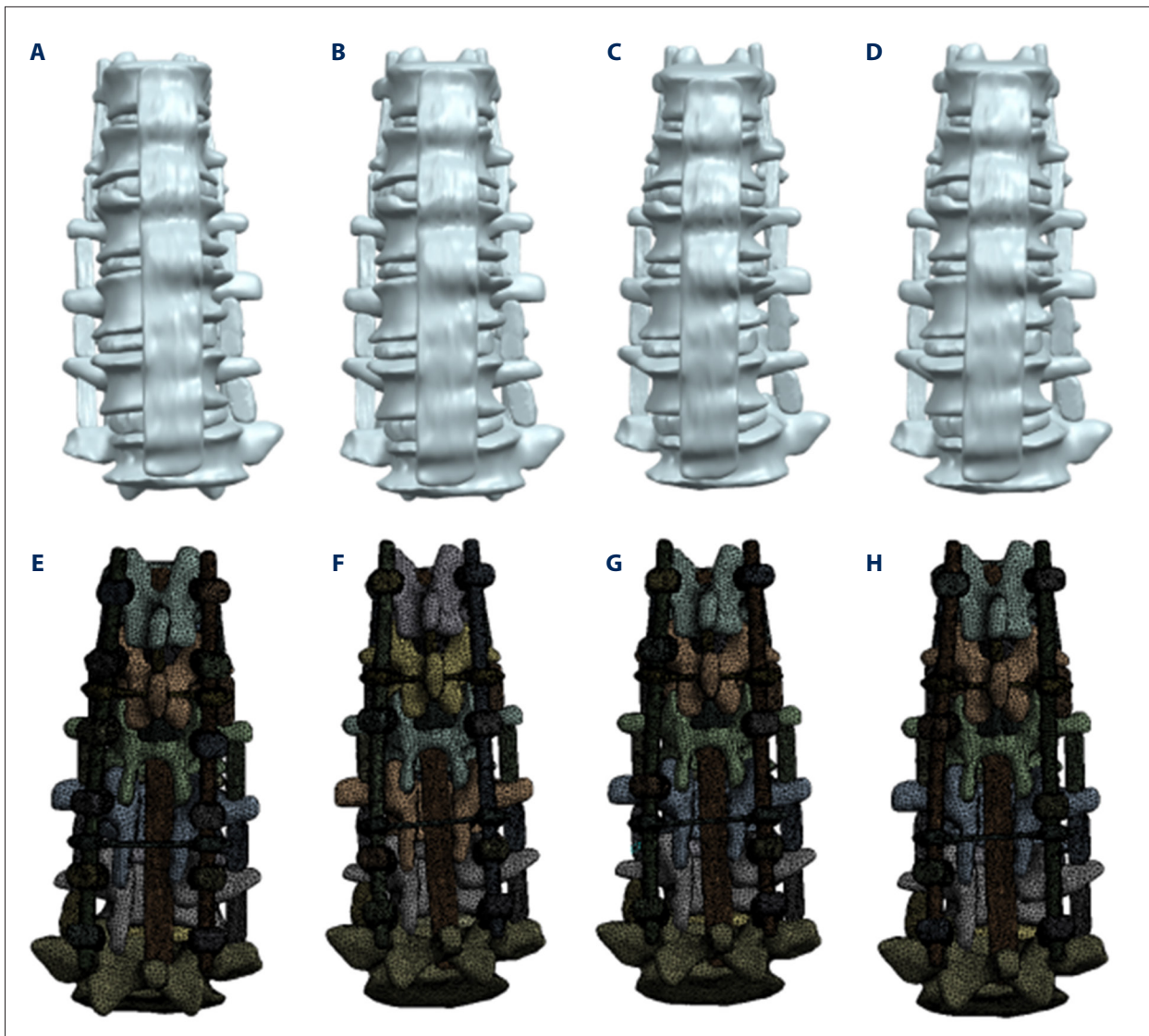


**Figure 2.** Establishment of 3D FE models of the full-segment, interval, key vertebra and strategic screw. (A–D) The full-segment (A), interval (B), key vertebra (C), and strategic (D) screw models were further polished and optimized by Geomagic Studio software. (E–H) Complete 3D FE models of the full-segment (E), interval (F), key vertebra (G), and strategic (H) screw by the Ansys software.

recognized values to confer the material properties of the lumbar spine [18], shown in Table 1. Finally, 4 sets of FE models were completely established (Figure 2E–2H).

### Main observation

Biomechanical characteristics of the screw-rod systems and intervertebral discs of the full-segment, interval, key vertebra, and strategic pedicle screw systems for the treatment of ADS were analyzed under 7 working conditions: upright, forward flexion, backward extension, left and right lateral bending, and left and right axial rotation. The degrees of freedom of the 5<sup>th</sup> lumbar vertebral body bottom surface at 6 directions

**Table 1.** Related material properties conferred to the FE models.

| Part                        | Modulus of elasticity (Mpa) | Poisson's ratio |
|-----------------------------|-----------------------------|-----------------|
| Screw-rod                   | 1.10E+05                    | 0.34            |
| Intervertebral disc annulus | 4.2                         | 0.45            |
| Vertebral body              | 1.20E+04                    | 0.3             |
| Ligament                    | 10                          | 0.3             |

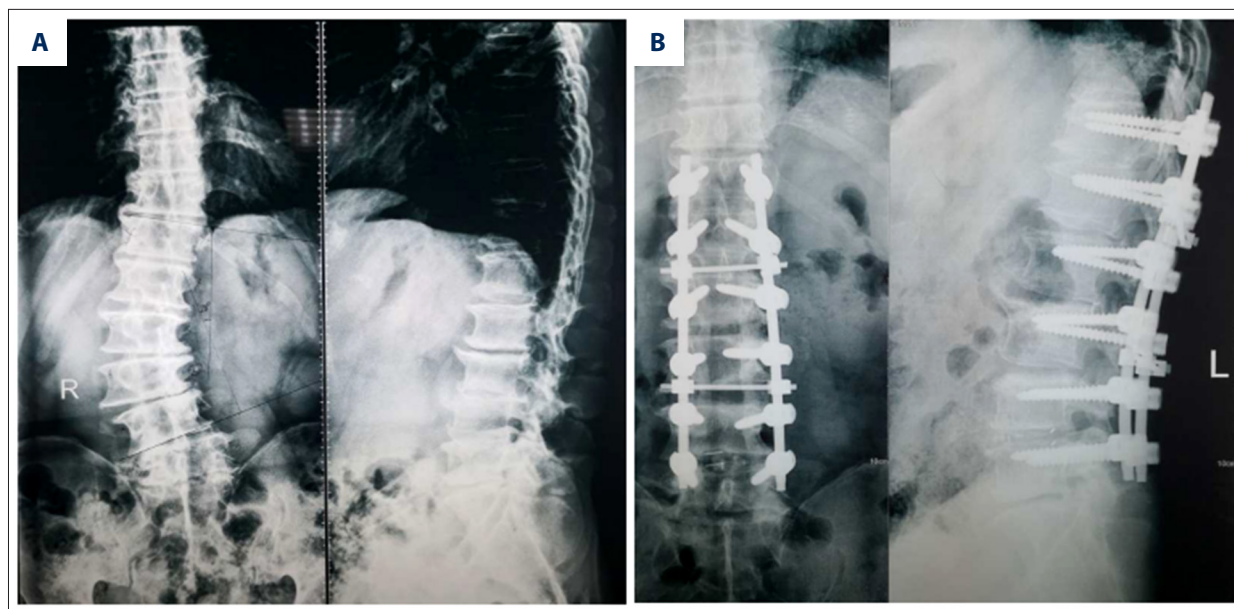


**Figure 3.** The X-ray images of spine (T12–L5) before (A) and after (B) operation.

were completely constrained, and force and moment were exerted on the center of the upper surface of the 12<sup>th</sup> thoracic vertebral body, including an axial load of 400 N applied to the models under various initial conditions (without the production of displacement) to simulate upright, forward flexion, backward extension, and left and right lateral bending, and a moment of 10 N/M applied under condition of left and right axial rotation [19]. The above values were imported into the Ansys16.1 software, and the stress of the 4 different pedicle screw schemes under 7 different working conditions were calculated and analyzed.

## Results

The patient received the internal fixation by pedicle screws after posterior incision in combination with subtotal laminectomy decompression and bone graft fusion. The X-ray images of the spine before and after the operation are shown in Figure 3.

Four sets of FE models were completely established, in which the full-segment fixation model had a total of 1 125 627 units and 1 708 211 nodes, the interval pedicle screw model 1 021 934 units and 1 548 315 nodes, the key vertebra model 1 021 948 units and 1 548 464 nodes, and the strategic model 997 735 units and 1 151 042 nodes. Forward flexion, backward extension, lateral flexion, and rotation greatly increased the force of the screw-rod systems (Tables 2, 3). Particularly, the force was more concentrated on the terminals of the head and tails of the screw-rod systems.

The maximum force values and positions of the screw-rod systems of 4 pedicle screw models under 7 different work conditions are shown in Figure 4 and summarized in Table 2. The maximum stress values for the full-segment pedicle screw system were lower than those for the interval, key vertebra, and strategic pedicle screw systems under almost all the working conditions except for the upright situation, as evidenced by darker colors of the model. Particularly, among all the systems except for the full-segment one, the key vertebra system caused minimum stress under upright, left, and right lateral flexion, and left and right axial rotation conditions.

The maximum force values of the vertebral bodies at L1, 2, 5, and T12 of the 4 pedicle screw models under 7 different work conditions are shown in Figure 5 and summarized in Table 3. Among these systems, the maximum force values of the vertebral body of the strategic pedicle screw system were the minimum under all the 7 working conditions, followed by those of the key vertebra and full-segment systems.

The maximum force values of vertebral bodies at T12–L5 of the 4 systems under 7 kinds of working conditions are shown in Tables 4–7. The maximum load of the full-segment, interval, and key vertebra pedicle screw systems under all the work conditions was at L2 (Tables 4–6). In contrast, for each vertebral body of the strategic pedicle screw system, the maximum load under upright condition was at L1, left and right axial rotation at T12, and forward flexion, backward extension, and left and right lateral flexion at L5 (Table 7).

**Table 2.** The maximum force values and positions of the screw-rod systems under 7 different work conditions of 4 screw models.

| Work condition        | Maximum stress values (Mpa) of different screw models |                                  |                                      |                                   |
|-----------------------|---|----------------------------------|--------------------------------------|-----------------------------------|
|                       | Full-segment screw system (position)                  | Interval screw system (position) | Key vertebra screw system (position) | Strategic screw system (position) |
| Upright               | 74.514 (L1, left)                                     | 75.782 (L2, left)                | 70.91 (L5, right)                    | 71.728 (T12, left)                |
| Forward flexion       | 463.04 (L5, right)                                    | 474.14 (L4, left)                | 492.58 (L5, right)                   | 537.74 (L5, right)                |
| Backward extension    | 455.44 (L5, right)                                    | 476.23 (L5, right)               | 501.74 (L5, right)                   | 550.16 (L5, right)                |
| Left lateral flexion  | 385.92 (L5, right)                                    | 486.37 (T12, left)               | 424.83 (T12, left)                   | 495.85 (T12, left)                |
| Right lateral flexion | 381.38 (L5, right)                                    | 563.88 (T12, left)               | 493.98 (T12, left)                   | 582.31 (T12, left)                |
| Left axial rotation   | 208.37 (T12, left)                                    | 333.39 (T12, left)               | 298.67 (T12, left)                   | 369.95 (T12, left)                |
| Right axial rotation  | 208.54 (T12, left)                                    | 333.43 (T12, left)               | 298.74 (T12, left)                   | 369.99 (T12, left)                |

L – lumbar vertebra; T – thoracic vertebra.

**Table 3.** The maximum force values at L1, 2, 5 or T12 of the vertebral bodies under 7 different work conditions of 4 screw models.

| Work condition        | Maximum stress values (Mpa) of different screw models |                                  |                                      |                                   |
|-----------------------|---|----------------------------------|--------------------------------------|-----------------------------------|
|                       | Full-segment screw system (position)                  | Interval screw system (position) | Key vertebra screw system (position) | Strategic screw system (position) |
| Upright               | 23.322 (L2)   | 26.484 (L2)                      | 22.131 (L2)                          | 13.46 (L1)                        |
| Forward flexion       | 259.77 (L2)   | 276.34 (L2)                      | 245.27 (L2)                          | 165.08 (L5)                       |
| Backward extension    | 257.14 (L2)   | 280.43 (L2)                      | 248.42 (L2)                          | 163.94 (L5)                       |
| Left lateral flexion  | 123.04 (L2)   | 154.79 (L2)                      | 120.39 (L2)                          | 110.59 (L5)                       |
| Right lateral flexion | 134.38 (L2)   | 177.75 (L2)                      | 139.26 (L2)                          | 109.74 (L5)                       |
| Left axial rotation   | 71.064 (L2)   | 98.844 (L2)                      | 82.07 (L2)                           | 48.425 (T12)                      |
| Right axial rotation  | 71.054 (L2)   | 98.836 (L2)                      | 80.053 (L2)                          | 48.404 (T12)                      |

L – lumbar vertebra; T – thoracic vertebra.

## Discussion

The main treatment method currently used for ADS is posterior spinal canal decompression and internal fixation using pedicle screws. There are controversies regarding the selection of long- and short- segment fixation [4–6]. Selective pedicle screw schemes with reduced screw numbers have been used with satisfactory results and decrease the risks of post-operative complications (such as pedicle screws-related soft tissue and neural injury and infection).

Selective pedicle screw schemes have been widely used in the treatment of adolescent idiopathic scoliosis. For example, key vertebral [20–22], strategic [23], and interval [21,24] pedicle screw schemes have been shown to be safe and effective for the treatment of adolescent idiopathic scoliosis. Until now, however, the optimized pedicle screw strategies involving fewer

screws, such as key vertebral and strategic screw schemes, have rarely been employed in ADS. This study evaluated the biomechanical stress of the internal fixation screws and vertebral bodies of the continuous (full) and non-continuous (selective) pedicle screw (including interval, key vertebral and strategy pedicle screw) schemes under different work conditions in ADS patient using FE analysis. Although a few studies used FE analysis to carry out the biomechanical analysis of ADS [14–17], there have been no FE analysis-based studies evaluating the biomechanical characteristics of pedicle screw schemes for ADS.

In this study, we used spinal CT imaging data of an ADS patient after whole-segment pedicle screw fixation to establish a full-segment screw model and secondary interval, key vertebra, and strategic screw models using FE analysis. Then, we carried out biomechanical analysis of the screw-rod systems and

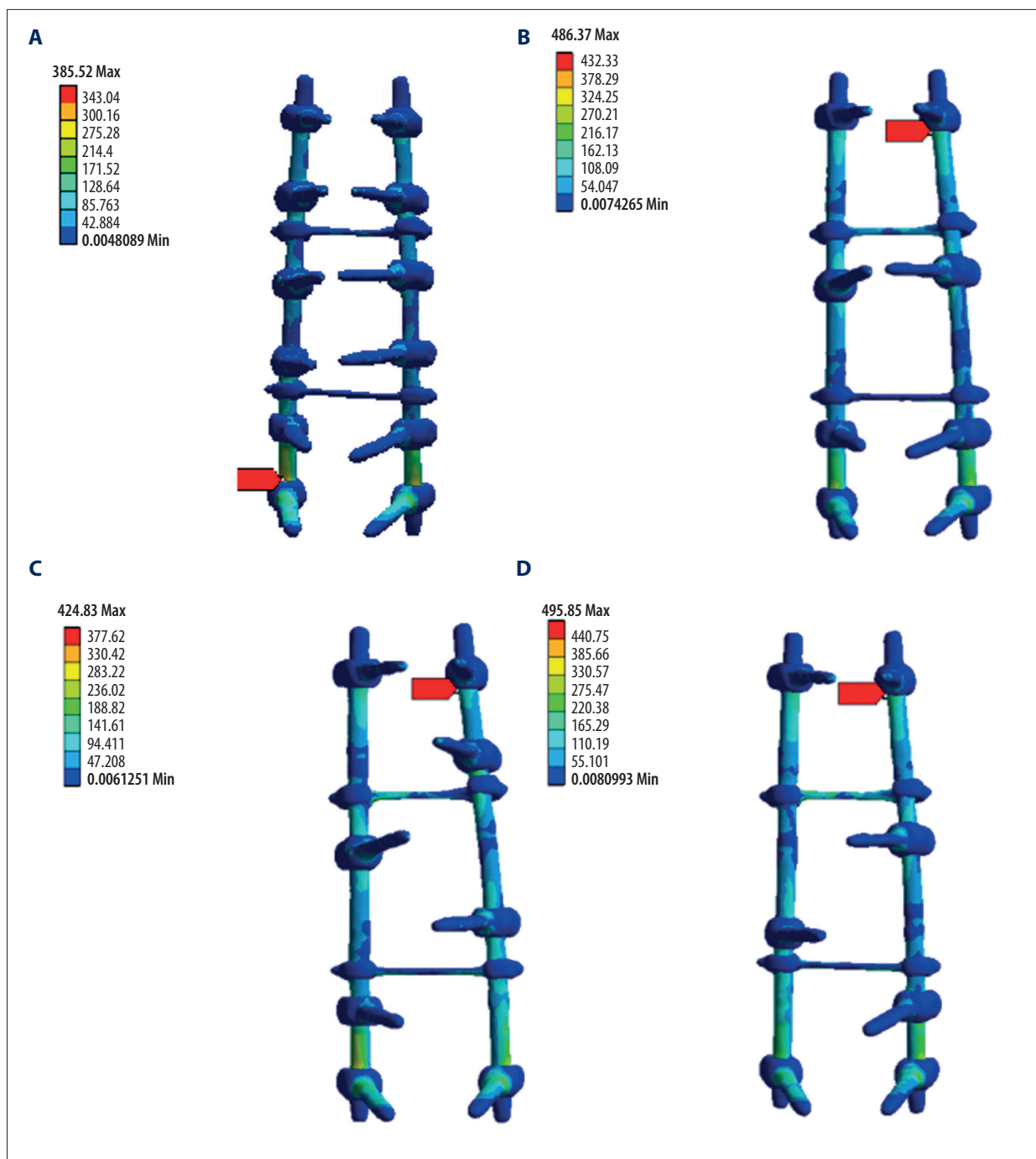


**Figure 4.** Typical biomechanical characteristics of the screw-rod systems of the full-segment (A), interval (B), key vertebra (C), and strategic (D) screw systems under left lateral flexion condition.

intervertebral discs of the 4 different screw schemes under 7 different working conditions (upright, forward flexion, backward extension, left and right lateral flexion, left and right axial rotation). Forward flexion, backward extension, lateral flexion, and axial rotation greatly increased the force of the screw systems and, particularly, the force was more concentrated on the terminals of the head and tails of the screw systems. Therefore, early

wearing of protective gears after the operation is particularly important, and patients should pay special attention to avoid these actions (especially forward flexion, backward extension, and lateral flexion) after healing. In addition, it is important to assure successful screw fixation in the screw-rod systems. If necessary, thicker pedicle screws should be used, which helps prevent fracture of the screw-rod systems after the operation.



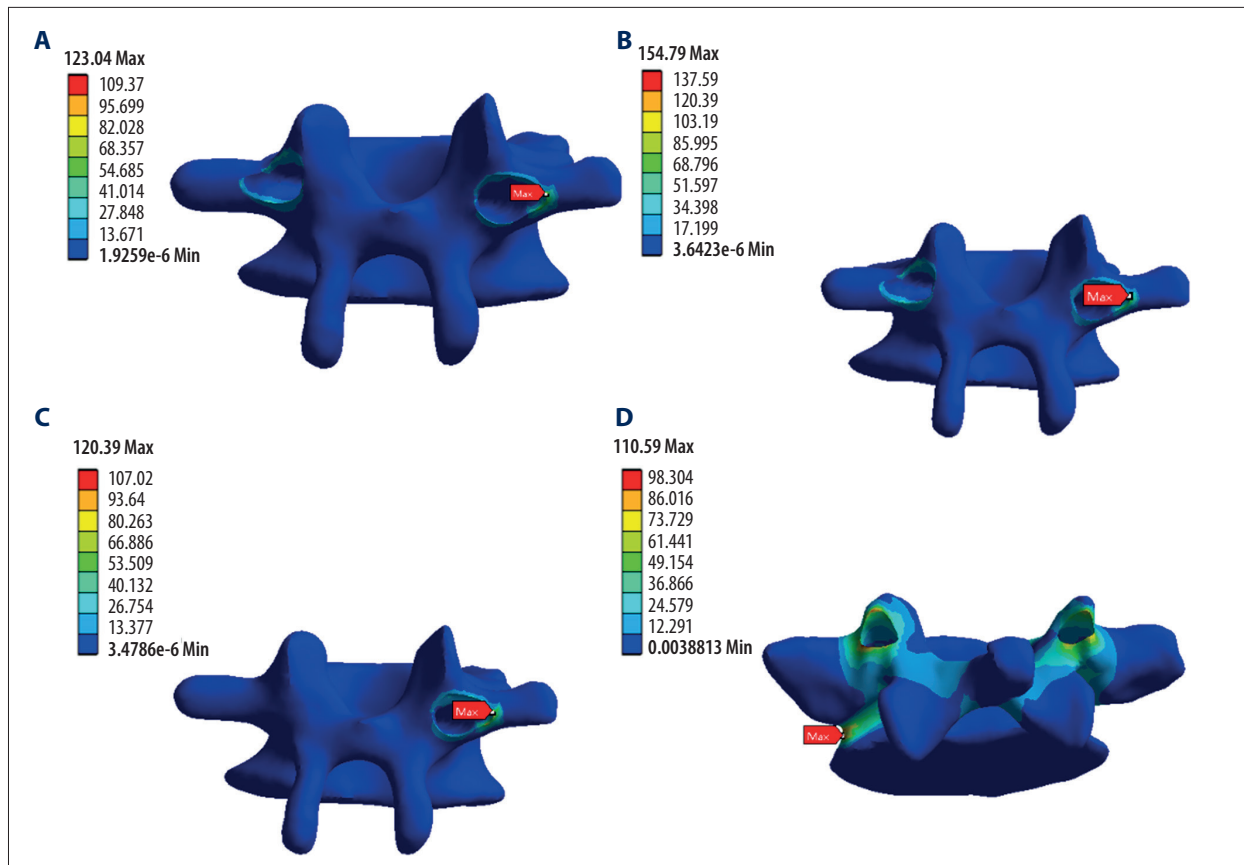


**Figure 5.** Typical biomechanical characteristics of the intervertebral discs of the full-segment (A, L2), interval (B, L2), key vertebra (C, L2), and strategic (D, L5) screw systems under left lateral flexion condition.

**Table 4.** Maximum force values of each vertebral body of the full-segment screw system under 7 working conditions.

| Work condition        | T12    | L1     | L2     | L3     | L4     | L5     |
|-----------------------|--------|--------|--------|--------|--------|--------|
| Upright               | 11.352 | 8.8407 | 23.322 | 4.6421 | 4.718  | 10.78  |
| Forward flexion       | 52.968 | 85.101 | 259.77 | 35.797 | 82.365 | 155.5  |
| Backward extension    | 52.523 | 83.705 | 257.1  | 97.161 | 84.25  | 156.75 |
| Left lateral flexion  | 61.531 | 63.217 | 123.04 | 98.032 | 74.676 | 108.62 |
| Right lateral flexion | 65.698 | 67.799 | 134.38 | 40.229 | 78.727 | 108.08 |
| Left axial rotation   | 29.276 | 29.284 | 71.064 | 22.952 | 28.952 | 24.208 |
| Right axial rotation  | 29.258 | 29.281 | 71.054 | 22.952 | 28.953 | 24.206 |

L – lumbar vertebra; T – thoracic vertebra.

The maximum stress values for the full-segment screw-rod system were lower than those for the interval, key vertebra, and strategic systems under almost all the working conditions except for the upright situation. In addition, the key vertebra screw system exhibited the second minimum stress under upright, left and right lateral flexion, and left and right axial rotation conditions. Among the 4 screw systems, the maximum force values of the vertebral bodies at L1, 2, 5, and T12 of the

strategic screw system were the minimum under all 7 working conditions, followed by those of the key vertebra and full-segment screw systems. This result suggests that the strategic and key vertebra screw systems can decrease the biomechanical stress of the screw-rod systems and vertebral bodies, which is close to that of the full-segment screw system. We found that the strategic and key vertebra screw systems, with fewer screws compared with the full-segment system, can reduce

**Table 5.** Maximum force values of each vertebral body of the interval screw system under 7 working conditions.

| Work condition        | T12    | L1     | L2     | L3      | L4     | L5     |
|-----------------------|--------|--------|--------|---------|--------|--------|
| Upright               | 12.502 | 15.54  | 26.484 | 0.39739 | 2.0029 | 10.27  |
| Forward flexion       | 57.259 | 92.638 | 276.34 | 1.7109  | 87.845 | 160.03 |
| Backward extension    | 57.899 | 91.527 | 280.43 | 1.7149  | 84.902 | 158.13 |
| Left lateral flexion  | 82.728 | 77.862 | 154.79 | 0.50366 | 90.264 | 109.13 |
| Right lateral flexion | 92.01  | 82.785 | 177.75 | 0.53707 | 96.997 | 108.4  |
| Left axial rotation   | 44.103 | 26.624 | 98.844 | 0.31245 | 33.852 | 26.666 |
| Right axial rotation  | 44.088 | 26.556 | 98.836 | 0.31244 | 33.856 | 26.663 |

L – lumbar vertebra; T – thoracic vertebra.

**Table 6.** Maximum force values of each vertebral body of the key vertebra screw system under 7 working conditions.

| Work condition        | T12    | L1     | L2     | L3     | L4     | L5     |
|-----------------------|--------|--------|--------|--------|--------|--------|
| Upright               | 11.697 | 10.045 | 22.131 | 4.3395 | 2.5735 | 10.438 |
| Forward flexion       | 60.064 | 95.599 | 245.27 | 69.288 | 66.354 | 174.95 |
| Backward extension    | 58.713 | 95.033 | 248.42 | 67.809 | 67.791 | 172.48 |
| Left lateral flexion  | 79.086 | 54.608 | 120.39 | 60.528 | 32.616 | 112.1  |
| Right lateral flexion | 87.67  | 51.58  | 139.26 | 63.863 | 36.716 | 114.46 |
| Left axial rotation   | 41.343 | 26.736 | 82.07  | 24.066 | 18.585 | 30.951 |
| Right axial rotation  | 41.317 | 26.558 | 82.053 | 24.072 | 18.59  | 30.951 |

L – lumbar vertebra; T – thoracic vertebra.

**Table 7.** Maximum force values of each vertebral body of the strategic screw system under 7 working conditions.

| Work condition        | T12    | L1     | L2     | L3     | L4     | L5     |
|-----------------------|--------|--------|--------|--------|--------|--------|
| Upright               | 12.328 | 13.46  | 7.5879 | 6.7443 | 3.6307 | 10.813 |
| Forward flexion       | 59.75  | 105.12 | 96.114 | 35.845 | 106.04 | 165.08 |
| Backward extension    | 60.463 | 104.11 | 93.714 | 37.514 | 103.9  | 163.94 |
| Left lateral flexion  | 88.287 | 99.606 | 90.765 | 32.563 | 94.484 | 110.59 |
| Right lateral flexion | 98.279 | 101.63 | 100.13 | 36.207 | 99.595 | 109.74 |
| Left axial rotation   | 48.425 | 25.272 | 43.915 | 18.8   | 25.136 | 32.186 |
| Right axial rotation  | 48.404 | 25.17  | 43.902 | 18.81  | 25.148 | 32.181 |

L – lumbar vertebra; T – thoracic vertebra.

biomechanical stress, screw instability, and discomfort in ADS patients in a similar way to the full-segment screw system, and can simultaneously decrease the postoperative complications (such as pedicle screws-related soft tissue and neural injury and infection) and control the medical costs.

For the full-segment, interval, and key vertebra screw systems, the maximum load under all the work conditions was at L2.

In contrast, for the strategic screw system, the maximum load of each vertebral body under upright condition was at L1, left and right axial rotation at T12, and forward flexion, backward extension, and left and right lateral flexion at L5. This indicates that when performing some kinds of screwing, we should pay more attention to specific spine segments with maximum load to avoid too much load-induced screw instability, and biomechanical stress, pain, and discomfort in patients.

There are several limitations to this study. First, the current FE method can only provide relatively accurate analysis of the internal fixed objects and vertebral bodies, and it is difficult to accurately simulate the soft tissue structures such as intervertebral discs, ligaments, and muscles. As a result, we might have failed to adequately simulate the biomechanical characters of screw schemes for the treatment of ADS, which might be solved by the development of computer technologies. Second, for ADS patients with severe osteoporosis, cement-augmented pedicle screws are commonly used, which might make it risky to use the key vertebral strategy and skip some of the levels unilaterally. This needs to be carefully evaluated in future studies. Third, cross-linking can increase the complexity of the biomechanical analysis of the spine, which was not evaluated in the present study. We plan to perform a FE-based biomechanical analysis in the presence and absence of cross-linking. Fourth, this study just involved a single ADS patient. In future research, we plan to assess cases of patients receiving various kinds of pedicle screw schemes, and FE analysis will be carried out to compare the biomechanical characteristics between healthy controls and ADS patients receiving the 4 kinds of pedicle screw schemes to further validate these results.

## References:

1. Silva FE, Lenke LG: Adult degenerative scoliosis: evaluation and management. *Neurosurg Focus*, 2010; 28(3): E1
2. Hong JY, Suh SW, Modi HN et al: The prevalence and radiological findings in 1347 elderly patients with scoliosis. *J Bone Joint Surg Br*, 2010; 92(7): 980–83
3. Schwab F, Dubey A, Gamez L et al: Adult scoliosis: prevalence, SF-36, and nutritional parameters in an elderly volunteer population. *Spine (Phila Pa 1976)*, 2005; 30(9): 1082–85
4. Faldini C, Di Martino A, Borghi R et al: Long vs. short fusions for adult lumbar degenerative scoliosis: Does balance matters? *Eur Spine J*, 2015; 24(Suppl. 7): 887–92
5. Kleinstueck FS, Fekete TF, Jeszenszky D et al: Adult degenerative scoliosis: Comparison of patient-rated outcome after three different surgical treatments. *Eur Spine J*, 2016; 25(8): 2649–56
6. Nishimura Y, Hara M, Nakajima Y et al: Outcomes and complications following posterior long lumbar fusions exceeding three levels. *Neurol Med Chir (Tokyo)*, 2014; 54(9): 707–15
7. Phan K, Xu J, Maharaj MM et al: Outcomes of short fusion versus long fusion for adult degenerative scoliosis: A systematic review and meta-analysis. *Orthop Surg*, 2017; 9(4): 342–49
8. Li J, Zhao Z, Tseng C et al: Selective fusion in Lenke 5 adolescent idiopathic scoliosis. *World Neurosurg*, 2018; 118: e784–91
9. Delfino R, Pizones J, Ruiz-Juretschke C et al: Selective anterior thoracolumbar fusion in adolescent idiopathic scoliosis: Long-term results after 17-year follow-up. *Spine (Phila Pa 1976)*, 2017; 42(13): E788–94
10. Direito-Santos B, Queirós CM, Serrano P et al: Long-term follow-up of anterior spinal fusion for thoracolumbar/lumbar curves in adolescent idiopathic scoliosis. *Spine (Phila Pa 1976)*, 2019; 44(16): 1137–43
11. Chang DG, Suk SI, Kim JH et al: Long-term outcome of selective thoracic fusion using rod derotation and direct vertebral rotation in the treatment of thoracic adolescent idiopathic scoliosis: More than 10-year follow-up data. *Clin Spine Surg*, 2020; 33(2): E50–57
12. Alizadeh M, Kadir MR, Fadhli MM et al: The use of X-shaped cross-link in posterior spinal constructs improves stability in thoracolumbar burst fracture: A finite element analysis. *J Orthop Res*, 2013; 31: 1447–54
13. Liao JC, Chen WP, Wang H: Treatment of thoracolumbar burst fractures by short-segment pedicle screw fixation using a combination of two additional pedicle screws and vertebroplasty at the level of the fracture: A finite element analysis. *BMC Musculoskelet Disord*, 2017; 18: 262
14. Haddas R, Xu M, Lieberman I et al: Finite element based-analysis for pre and post lumbar fusion of adult degenerative scoliosis patients. *Spine Deform*, 2019; 7(4): 543–52
15. Xu M, Yang J, Lieberman I et al: Finite element method-based study for effect of adult degenerative scoliosis on the spinal vibration characteristics. *Comput Biol Med*, 2017; 84: 53–58
16. Wang L, Zhang B, Chen S et al: A validated finite element analysis of facet joint stress in degenerative lumbar scoliosis. *World Neurosurg*, 2016; 95: 126–33
17. Zheng J, Yang Y, Lou S et al: Construction and validation of a three-dimensional finite element model of degenerative scoliosis. *J Orthop Surg Res*, 2015; 10: 189
18. Wang X, Dumas GA: Evaluation of effects of selected factors on intervertebral fusion – a simulation study. *Med Eng Phys*, 2005; 27(3): 197–207
19. Lenke LG, Betz RR, Harms J et al: Adolescent idiopathic scoliosis: A new classification to determine extent of spinal arthrodesis. *J Bone Joint Surg Am*, 2001; 83(8): 1169–81
20. Li J, Cheung KM, Samartzis D et al: Key-vertebral screws strategy for main thoracic curve correction in patients with adolescent idiopathic scoliosis. *Clin Spine Surg*, 2016; 29(8): E434–41
21. Wang F, Xu XM, Lu Y et al: Comparative analysis of interval, skipped, and key-vertebral pedicle screw strategies for correction in patients with Lenke type 1 adolescent idiopathic scoliosis. *Medicine (Baltimore)*, 2016; 95(10): e3021
22. Wei XZ, Zhou XY, Yang YL et al: Key vertebral pedicle screw strategy for the correction of flexible Lenke type 1 adolescent idiopathic scoliosis: A preliminary study of a 5-year minimum radiographic follow-up. *Spine (Phila Pa 1976)*, 2017; 42(16): 1226–32
23. Dumpa SR, Shetty AP, Aiyer SN et al: Reciprocal changes in sagittal alignment in adolescent idiopathic scoliosis patients following strategic pedicle screw fixation. *Asian Spine J*, 2018; 12(2): 300–8
24. Ohrt-Nissen S, Kamath VHD, Samartzis D et al: Fulcrum flexibility of the main curve predicts postoperative shoulder imbalance in selective thoracic fusion of adolescent idiopathic scoliosis. *Eur Spine J*, 2018; 27(9): 2251–61

## Conclusions

The full-segment screw system is recommended for the surgical treatment of ADS patients, with good physical and economical conditions. The strategic and key vertebra screw systems can reduce the biomechanical stress and instability of screw-rod systems and vertebral bodies in a similar way to the full-segment screw system. In clinical practice, we can choose a reasonable screw scheme according to the actual situation of patients. Our present results may help in further research on optimal surgical procedures based on different conditions during pedicle screw fixation, which can maximally reduce the risk of postoperative complications after screwing and simultaneously maintain reasonable 3D orthopedic results.

## Acknowledgements

We thank Dr. Xiu Zhong for helping collect the CT images and Dr. Ming Su for help in the establishment and analysis of the finite element model.

## Conflict of interest

None.